

Supporting Information

Mechanochemical synthesis of AIE-TICT-ESIPT active orange-emissive chemodosimeter for selective detection of hydrogen peroxide in aqueous media and living cells, and solid-phase quantitation using a smartphone

Akhil A. Bhosle,^a Mainak Banerjee,^{*a} Varsha Gupta,^b Surajit Ghosh,^{b,c} Achikanath C. Bhasikuttan,^{d,e} Amrita Chatterjee^{*a}

^aDepartment of Chemistry, BITS Pilani, K. K. Birla Goa Campus, NH 17B Bypass Road, Zuarinagar, Goa 403726, INDIA

^bCSIR-Indian Institute of Chemical Biology, Jadavpur, Kolkata 700032, INDIA

^cDepartment of Bioscience & Bioengineering, Indian Institute of Technology Jodhpur, NH 62, Surpura Bypass Road, Karwar 342037, Rajasthan, India

^dRadiation & Photochemistry Division, Bhabha Atomic Research Centre, Trombay, Mumbai, INDIA

^eHomi Bhabha National Institute, Anushaktinagar, Mumbai, INDIA

Table of Contents

Sr. No.	Contents	Page No.
1.	Experimental procedures	S2-S5
2.	The absorption and emission maxima of BTPA in various solvents (Table S1)	S6
3.	Quantum yields of BTPA in different solvents (Table S2)	S6
4.	Fluorescence responses of BTPA in different solvent systems (Fig. S1)	S7
5.	Particle size and SEM analysis of BTPA in DMSO-H ₂ O fractions (Fig. S2)	S8
6.	Viscometric fluorescence change of BTPA in glycerol-methanol (Fig. S3)	S8
7.	pH study of BTPA , BTPAB in the absence and presence of H ₂ O ₂ (Fig. S4)	S9
8.	Fluorescence responses of BTPAB in DMSO-Water solvent systems (Fig. S5)	S9
9.	Time-dependent study for BTPAB upon addition of H ₂ O ₂ (Fig. S6)	S10
10.	UV-vis responses of BTPAB in the presence and absence of H ₂ O ₂ (Fig. S7)	S10
11.	Bar diagrams of selectivity of BTPAB against various ROS, cations, anions, other species (Fig. S8-11)	S11-S12
12.	¹ H NMR spectra of BTPAB after reaction with H ₂ O ₂ (Fig. S12)	S13
13.	Life-time decay trace of BTPAB with different concentrations of H ₂ O ₂ (Table S3)	S13
14.	MTT assay of BTPAB (Fig. S13)	S14
15.	Comparative table of different AIE based probes for H ₂ O ₂ sensing (Table-S4)	S15-S21
16.	References	S22-S24
17.	¹ H and ¹³ C NMR Spectra	S25-S28

1. Experimental procedures

Chemicals and reagents

2-Aminothiophenol, 5-chlorosalicylaldehyde, hexamethylenetetramine, TFA, benzophenone hydrazone, 4-(bromomethyl)phenylboronic acid, H₂O₂, etc., were purchased from TCI or Sigma-Aldrich chemicals. The procurement of AR-grade solvents and all other common chemicals was done from different commercial suppliers and used without further purification. 0.25 mm silica gel plates (60F-254) were used to monitor the reactions using thin-layer chromatography (TLC) and visualized under UV light (254 or 365 nm). The ultrapure deionized water was collected from Millipore water system (18 MΩ.cm) and purged with N₂ for 15 min before the analytical study.

Instrumentation and measurements

The mechanochemical reactions were carried out in a RETSCH MM400 mixer mill or an indigenous automated Agate mortar-pestle (Scientific instruments, India). Bruker Avance (400 MHz or 500 MHz) NMR spectrometer was used to record the NMR spectra of the synthesized compounds. QTOF LC-MS (6545 Q-TOF LC-MS, Agilent) was used for the acquisition of HRMS spectra. For UV-vis absorption spectra, JASCO V-550 was used, and the data pitch and bandwidth were set as 1 nm. Fluorescence spectra were taken on a JASCO FP-8500 spectrofluorometer; the slit width was 2.5 nm for both excitation and emission. The time-resolved fluorescence measurements were carried out using a time-correlated single-photon-counting (TCSPC) spectrometer (Horiba Jobin Yvon IBH, UK). Particulate system NanoPlus zeta/nano particle analyzer was used for the DLS study. Solid-phase detection was demonstrated on 0.25 mm silica gel coated TLC plates and images were captured on a Xiaomi Mi10i smartphone (108 megapixels) without filters.

Analytical procedure

1 mM stock solution of **BTPAB** was prepared in DMSO and diluted further using phosphate buffer saline (PBS) (10 mM, pH 7.4). All spectrofluorimetric studies were carried out using 10 μ M **BTPAB** solution in 1% DMSO in PBS as the solvent system. 1 mM stock solution of H₂O₂ was prepared in PBS and used. Similarly, for selectivity studies, the stock solutions (1 mM) of different peroxides, amino acids, oxidizing, and reducing agents were prepared in PBS and used. For cations nitrates (or chlorides) salts and for anions sodium (or potassium) salts were taken to make 1 mM stock solutions in PBS. The fluorescence responses upon the addition of 20 equiv (200 μ M) of the various analytes to 10 μ M **BTPAB** solution were recorded to study the selectivity of **BTPAB** towards H₂O₂. The excitation wavelength was kept at 384 nm, and the emission intensities were examined over a range from 385 nm to 750 nm. The pH study was carried out by preparing different buffer solutions ranging from pH 3-5 in 0.1 M acetate buffer, pH 6-8 in 10 mM PBS buffer, and pH 9-10 in 0.1 M carbonate buffer. For real sample analysis, the solutions were prepared by spiking known concentrations of H₂O₂ in a water sample collected from various local water bodies and in the blood serum sample of a healthy female donor. Analytical solutions were filtered through syringe filters of 0.22 μ m to remove any particulate matter before fluorescence measurements. All the analysis were carried out at room temperature (25 °C), repeated thrice and the average data was reported.

Fluorescence quantum yield calculation

Fluorescence quantum yield was calculated using the equation:

$$\varphi_x = \varphi_{std} \times \frac{I_x}{I_{std}} \times \frac{A_{std}}{A_x} \times \frac{n_x^2}{n_{std}^2}$$

where ϕ = quantum yield, I = emission intensity, η = refractive index and A = optical density. The standard 2-hydroxybenzothiazole (HBT) is represented as subscript 'std' and 'x' denotes BTPA.¹

Preparation of various ROS and RNS species²

ONOO⁻

ONOO⁻ was prepared by adding HCl (0.6 M, 10 mL) to a vigorously stirred solution of NaNO₂ (0.6 M, 10 mL) and H₂O₂ (0.7 M, 10 mL) in deionized H₂O at 0 °C. To this mixture, NaOH (1.5 M, 20 mL) was added immediately and the excess hydrogen peroxide was removed by passing the solution through a short column of MnO₂. Aliquots of the solution were stored at -20 °C for use.

NO

To a stirred solution of NaNO₂ (7.3 M), H₂SO₄ (3.6 M) was added dropwise and the emitted gas was allowed to pass through a solution of NaOH (2 M) first and then deionized H₂O to make a saturated NO solution of 2.0 mM.

¹O₂

Equal aliquots of NaMoO₄ (10 mM) and H₂O₂ (10 mM) prepared in PBS (10 mM, pH 7.4) were mixed to yield ¹O₂ of 5 mM.

·OH

To a solution of H₂O₂ (1.0 mM, 1.0 mL) in PBS (10 mM, pH 7.4) was added to FeSO₄ solution (1.0 mM, 100 μL) at ambient temperature and ·OH was generated by Fenton reaction (stock solution 0.1 mM).

O₂^{·-}

KO₂ was dissolved in dry DMSO to make a saturated solution of O₂^{·-} (stock solution 1 mM).

Cell culture and cytotoxicity assay

Hela cells were cultured in a low glucose DMEM medium supplemented with 10% FBS and 1% penicillin-streptomycin solution in an incubator with 5% CO₂ at 37 °C temperature. MTT assay was performed to check the viability of the cells after the treatment with the probe. For this, Hela cells were seeded in 96 well plates and incubated at 37 °C. After the cells reached 70% confluency treatment was given at different doses (100, 50, 25, 12.5, 6.25, 3.12, and 1.56 μM). After 24 h of treatment, MTT (3-(4,5-Dimethylthiazol-2-Yl)-2,5-Diphenyltetrazolium bromide) solution was added to each well at 5 mg/mL concentration and incubated for 4 h. After reduction of MTT, the obtained formazan was dissolved using a 1:1 DMSO-methanol solution, and absorbance was taken at 550 nm in a plate reader.

Cell imaging

Cells were seeded in 35 mm glass-bottom confocal dishes. When confluency reached, cells were treated with 5 μM and 10 μM of the probe and incubated for 30 min. After this, cells were washed with PBS and treated with 50 μM H₂O₂. Imaging was done at 15 min and 30 min time points to check the fluorescence intensity using a fluorescence microscope (Olympus IX80) under the 40X objective.

Blood serum sample preparation³

The human blood serum of a healthy donor (female) was collected from the medical center of the same institute and stored at -20 °C. The serum samples were spiked with different levels of H₂O₂ and were centrifuged for 30 min (maintaining a low temperature). The supernatant was collected, and for each mL of the supernatant, 3 mL of acetone was added. Proteins precipitated at this stage were further centrifuged for 10 min; after that, the supernatant was collected and

diluted with a measured volume of Millipore water. The contaminated serum sample with H₂O₂ was used to carry out the fluorescence study.

2. Table S1. UV-vis absorption and emission wavelengths of **BTPA** in different solvents.

Solvent	UV-vis absorption (λ_{ab})	Emission (λ_{em})	Stokes Shift (nm)
DMF	313 nm, 360 nm, 494 nm	615 nm	255
DMSO	314 nm, 362 nm, 498 nm	617 nm	255
THF	308 nm, 347 nm, 416 nm	605 nm	258
MeOH	307 nm, 370 nm, 423 nm	617 nm	247
EtOH	309 nm, 374 nm, 427 nm	616 nm	242

3. Table S2. Quantum yields of **BTPA** in different solvents.

Solvent	λ_{ab} (nm)	λ_{em} (nm)	Φ_F
THF	347	605	0.3932
MeOH	370	617	0.3134
EtOH	374	616	0.3372

4. Fluorescence responses of BTPA in different solvent systems

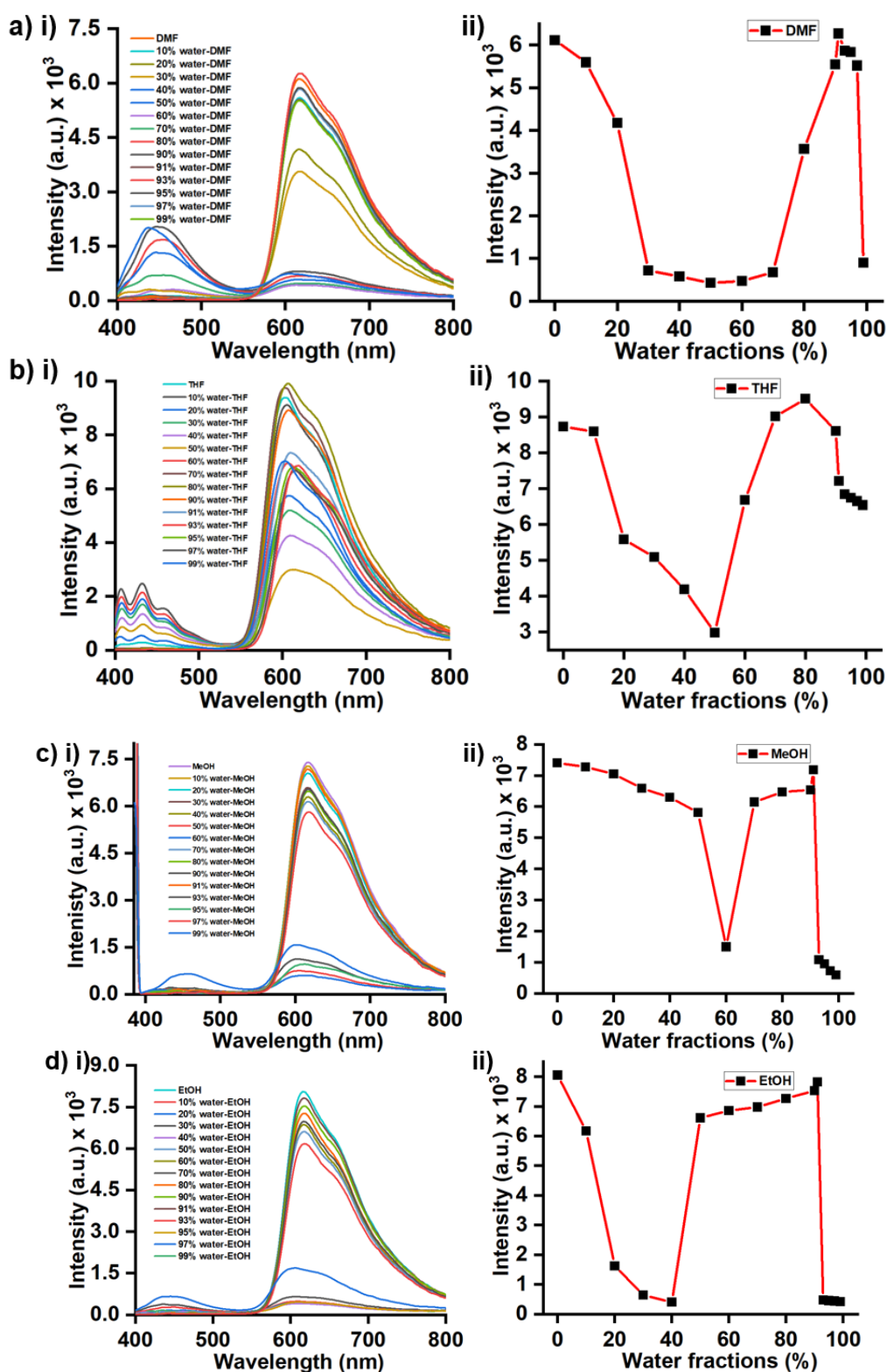


Fig. S1 Fluorescence response of various water-organic solvent fractions: a) DMF-water, b) THF-water, c) Methanol-water, and d) Ethanol-water fraction for (i) emission of 10 μM **BTPA** and (ii) a plot of change in the relative fluorescence intensity of **BTPA** at 617 nm as a function of different water fractions ($\% f_w$).

5. Particle size analysis of BTPA in DMSO-H₂O fractions

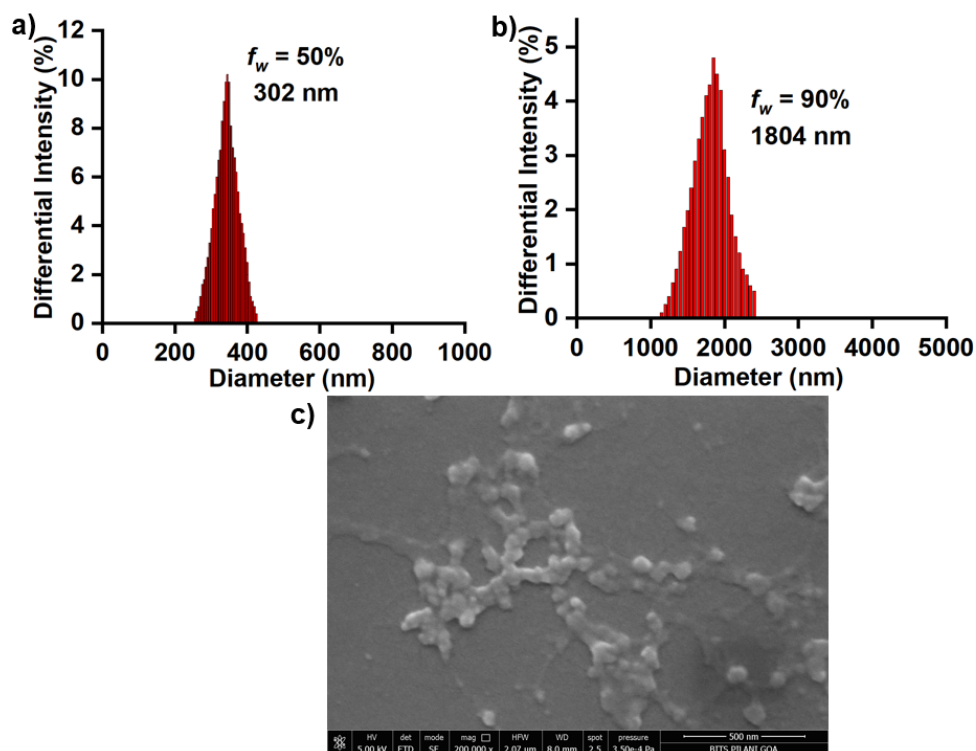


Fig. S2 Particle size analysis of **BTPA** in (i) 1:1 DMSO-H₂O, (ii) 1:9 DMSO-H₂O fractions and SEM image of **BTPA** in 1:9 DMSO-H₂O fraction.

6. Viscometric fluorescence change of BTPA in glycerol-methanol

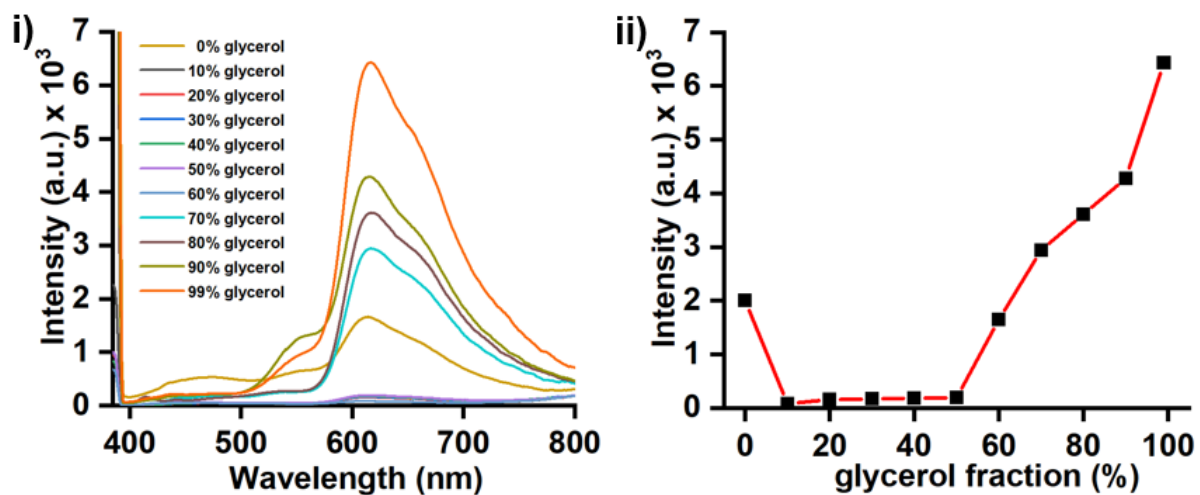


Fig. S3 a) Fluorescence response of **BTPA** (10 μ M) at varying MeOH–glycerol fraction (λ_{ex} 384 nm). b) Change in the relative fluorescence intensity of **BTPA** at 617 nm as a function of different percentages of the glycerol fraction (% f_w).

7. pH study of BTPA, BTPAB in the absence and presence of H₂O₂

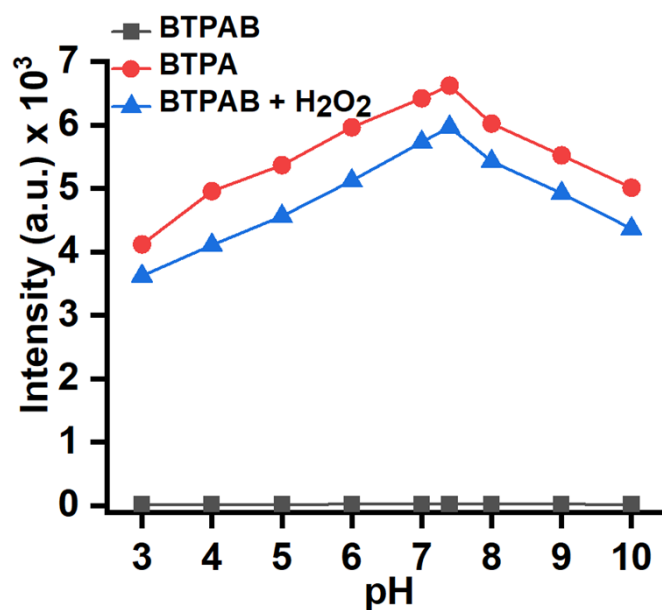


Fig. S4 Effect of pH on the relative emission intensities of **BTPA** and **BTPAB** (10 μ M in 1% DMSO:PBS (10 mM, pH 7.4) at 617 nm in the absence and the presence of 10.0 equiv of H₂O₂ ions (λ_{ex} 384 nm; λ_{em} 617 nm).

8. Fluorescence response of BTPAB at different of H₂O₂

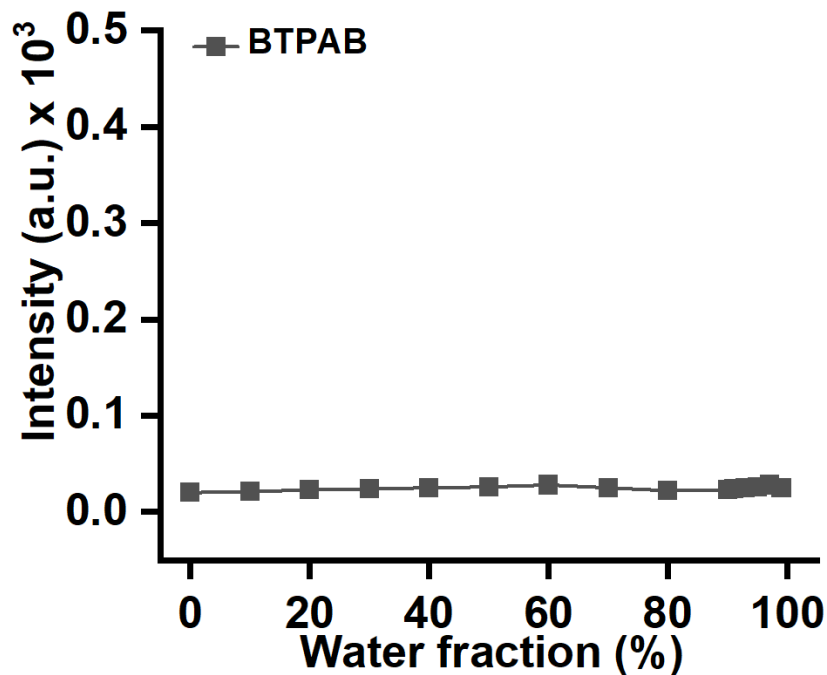


Fig. S5 Fluorescence response of **BTPAB** at 617 nm as a function of different DMSO-water fractions (% f_w).

9. Time-dependent study for BTPAB upon addition of H₂O₂

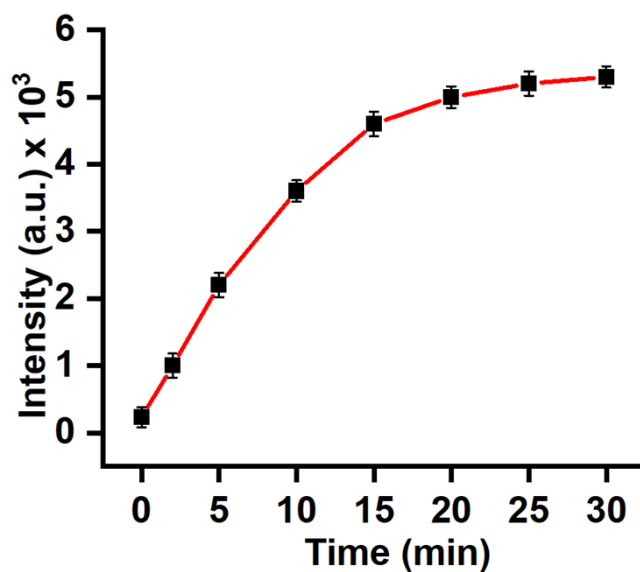


Fig. S6 Time-dependent study and effect on the relative emission intensities of **BTPAB** (10 μ M in 1% DMSO:PBS (10 mM, pH 7.4) upon addition of 10 equiv of H₂O₂; λ_{ex} 384 nm; λ_{em} 617 nm).

10. UV-vis responses of BTPAB in the presence and absence of H₂O₂

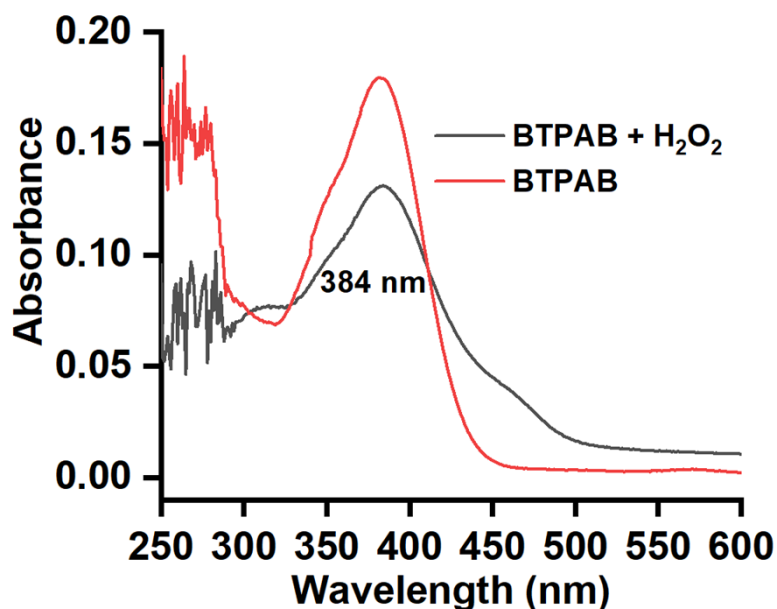


Fig. S7 The UV-Vis responses of **BTPAB** (10 μ M) in the presence and the absence of H₂O₂ (100 μ M) showed no significant change in the absorption band at 384 nm.

11. Bar diagrams of selectivity of BTPAB against various ROS, cations, anions, other species

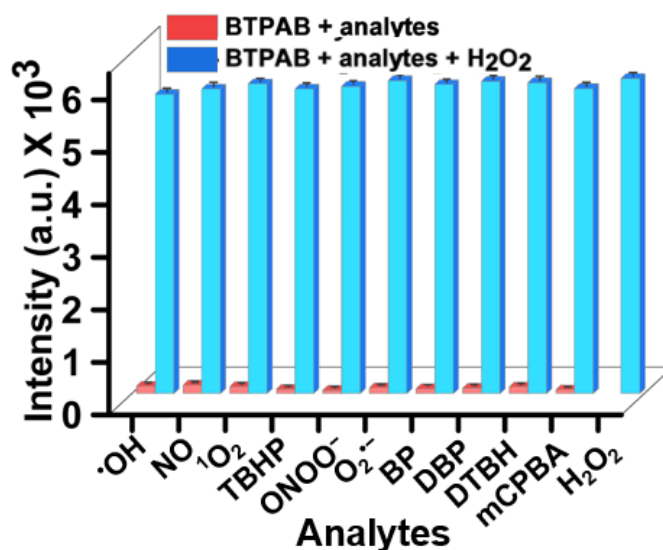


Fig. S8 The fluorimetric responses of various ROS (200 μ M) towards **BTPAB** (10 μ M in 1% DMSO in PBS (10 mM), pH 7.4; (λ_{ex} 384 nm; λ_{em} 617 nm) and the fluorimetric responses of **BTPAB** + reactive oxygen species upon addition of H₂O₂.

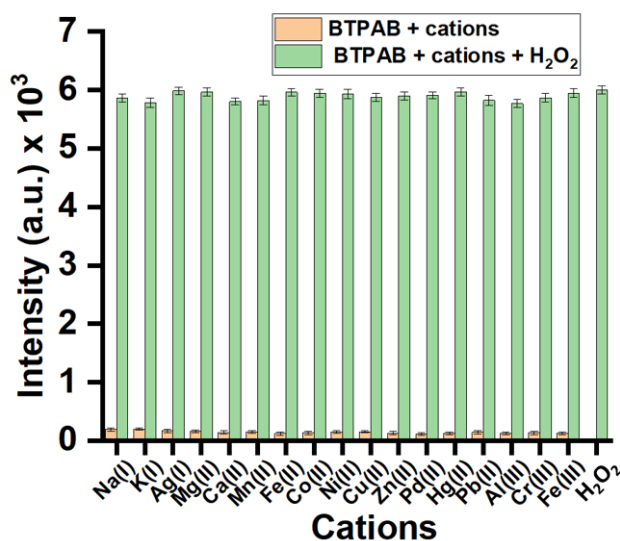


Fig. S9 The fluorimetric responses of various cations (200 μ M) towards **BTPAB** (10 μ M in 1% DMSO in PBS (10 mM), pH 7.4; (λ_{ex} 384 nm; λ_{em} 617 nm) and the fluorimetric responses of **BTPAB** + cations upon addition of H₂O₂.

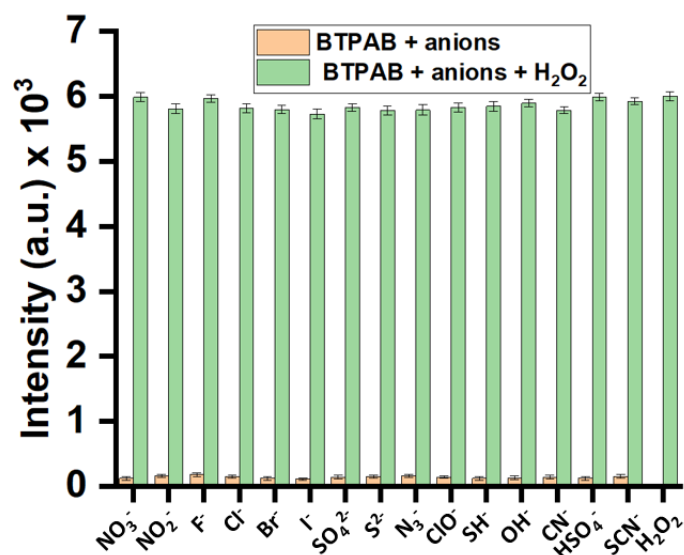


Fig. S10 The fluorimetric responses of various anions (200 μM) towards **BTPAB** (10 μM in 1% DMSO in PBS (10 mM), pH 7.4; (λ_{ex} 384 nm; λ_{em} 617 nm) and the fluorimetric responses of **BTPAB** + anions upon addition of H_2O_2 .

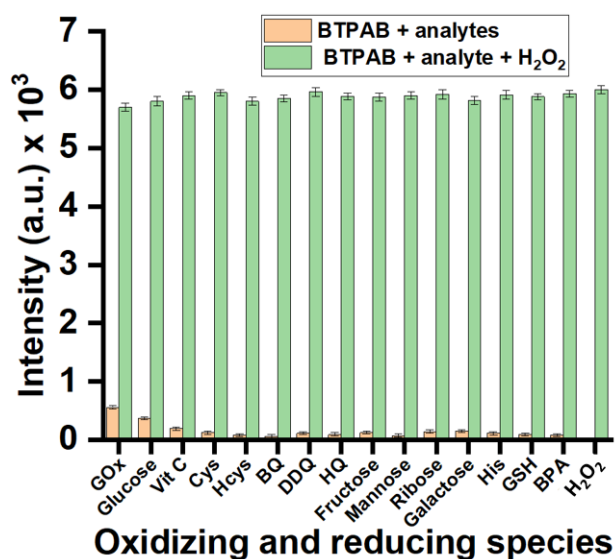


Fig. S11 The fluorimetric responses of various oxidizing and reducing species (200 μM) towards **BTPAB** (10 μM in 1% DMSO in PBS (10 mM), pH 7.4; (λ_{ex} 384 nm; λ_{em} 617 nm) and the fluorimetric responses of **BTPAB** + oxidizing and reducing species upon addition of H_2O_2 .

12. NMR spectra of BTPAB in presence of H₂O₂ to afford BTPA

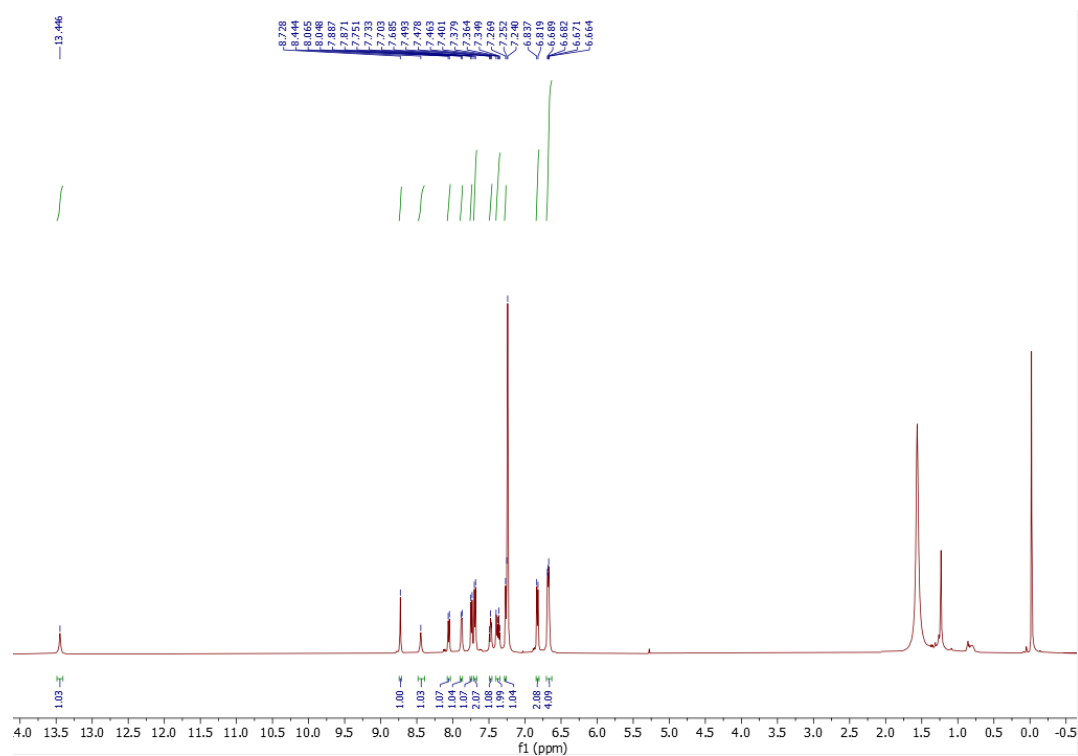


Fig. S12 ¹H NMR spectra of the probe **BTPAB** upon reaction with H₂O₂ to give the precursor **BTPA**.

13. Table S3. Life-time decay trace of BTPAB and BTPAB with different concentrations of H₂O₂.

Entry	τ_1 /ns (% contribution)	τ_2 /ns (% contribution)	τ_3 /ns (% contribution)	χ^2	τ_{av}
10 μ M BTPAB	1.7774 (49)	0.6588 (15)	0.3885 (36)	1.02	0.94
10 μ M BTPAB + 50 μ M H ₂ O ₂	0.8965 (26)	2.9218 (74)	----	1.14	1.91
10 μ M BTPAB + 100 μ M H ₂ O ₂	0.0479 (14)	5.2155 (86)	----	0.91	2.63
BTPA	0.8675 (20)	4.6325 (80)	----	1.11	2.75

14. MTT assay of BTPAB

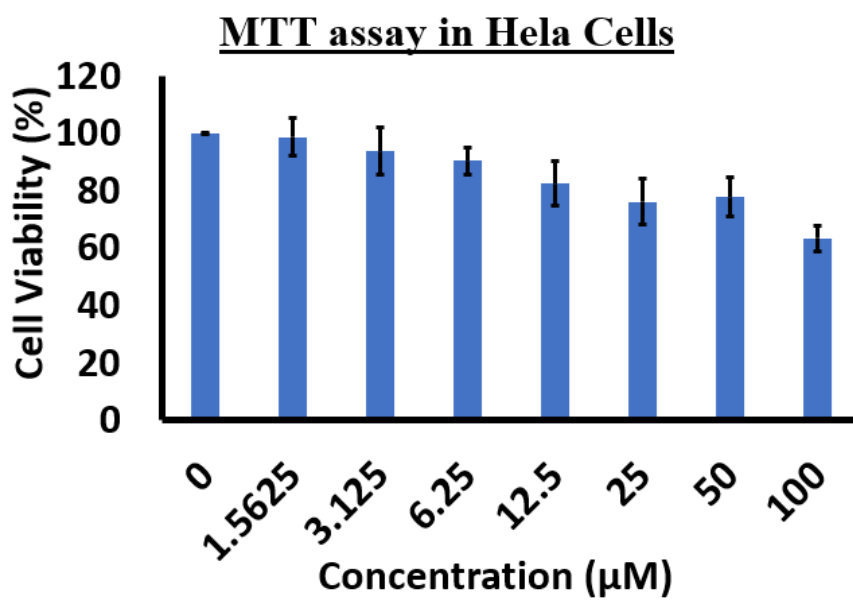
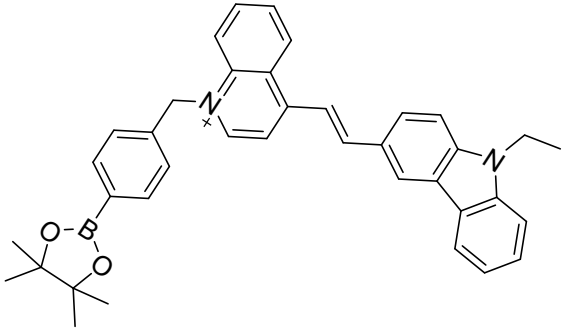
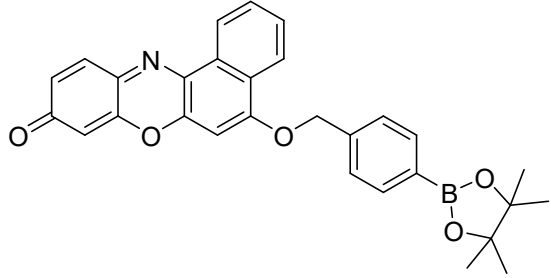
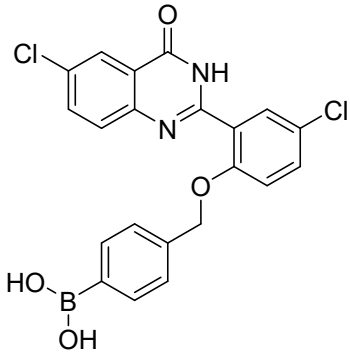
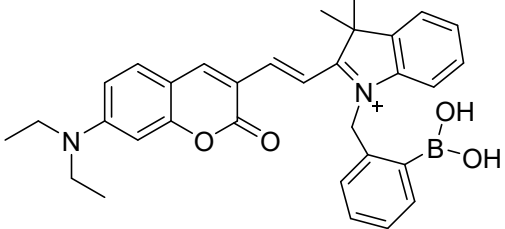
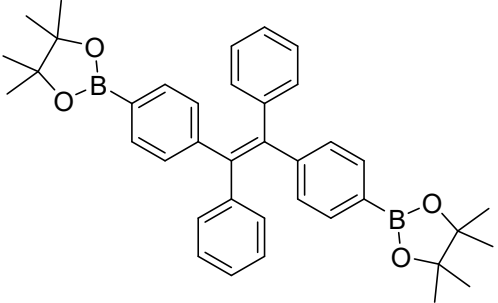


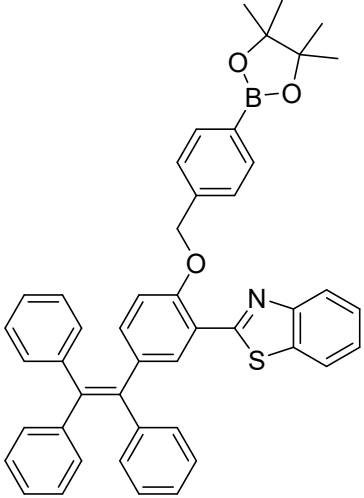
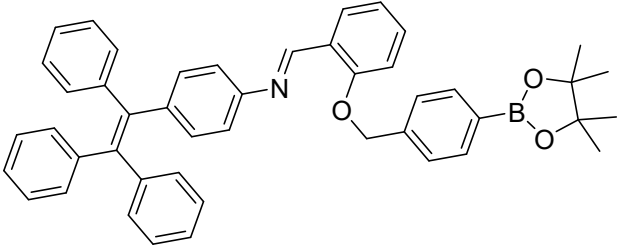
Fig. S13 Cell viability (bar-chart) of BTPAB.

15. Table S4. Comparison of various available AIE, ESIPT fluorescent probes for hydrogen peroxide sensing.

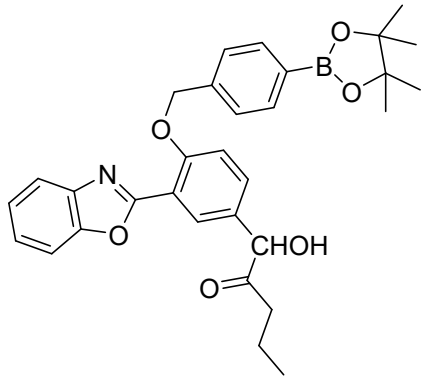
Sr. No.	Sensors	Photo-physical properties	medium	$\lambda_{ex}/\lambda_{em}$	LOD; linearity range	Cell study	Solid-phase sensing	Real Sample	Reference
1	 <p>3-steps synthesis Key reagents: Carbazole, 4-methyl quinoline, piperidine, 4-(Bromomethyl) benzene boronic acid pinacol ester, POCl₃, NaH, iodoethane. Media: DMF, Ethanol, Toluene.</p>	PET	DMSO/PBS buffer (01:99, v:v)	376 nm; 527 nm ↑	0.2-10.0 μM; 0.04 μM	Yes	No	No	4

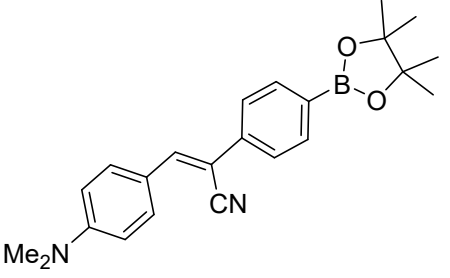
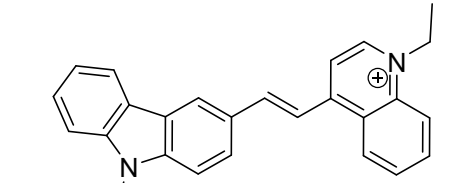
2	 <p>3-steps synthesis Key reagents: Resorcinol, 1-naphthol, 4-(Bromomethyl)- benzene boronic acid pinacol ester. Media: CH₂Cl₂, HCl, DMF.</p>	PET	DMSO/PBS buffer (01:99, v:v)	570 nm; 638 nm ↑	0-140 μM; 0.091 μM	Yes	No	No	5
3	 <p>3-steps synthesis Key reagents: 2-amino-5-chlorobenzamide, bis(pinacolato)diboron, Pd(dppf)Cl₂. Media: DMF, Ethanol, DMA.</p>	ESIPT	-	365 nm; 525 nm ↑	-; -	Yes	No	No	6

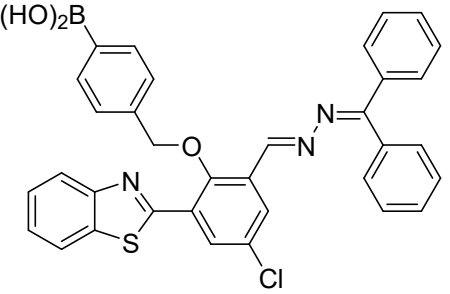
4	 <p>2-steps synthesis</p> <p>Key reagents: 7-(diethylamino)-2-oxo-2H-chromene-3-carbaldehyde, 3-methyl-butan-2-one, 2-(bromomethyl) phenylboronic acid, Media: Acetic acid, CH₃CN, ethanol.</p>	ICT	DMSO/PBS buffer (01:99, v:v)	410 nm, 590 nm; 522 nm ↑, 670 nm ↓	3.3 μM; 0.99	Yes	No	No	7
5	 <p>2-steps synthesis</p> <p>Key reagents: 4-bromobenzophenone, Zn, TiCl₄, bis(pinacolato)diboron, Pd(dppf)Cl₂. Media: THF, DMF.</p>	AIE	-	400 nm; 500 nm ↑	0-200 μM; 0.52 μM	Yes	No	No	8

6	 <p>2-steps synthesis from TPE-OH-CHO Key reagents: 2-amino thiophenol, 4-(Bromomethyl)- benzene boronic acid pinacol ester, HCl, H₂O₂. Media: EtOH, DMF.</p>	AIE	DMF/PBS buffer (1:1, v:v)	380 nm; 550 nm ↑	0-100 μM; 6 μM	Yes	No	No	9
7	 <p>3-steps synthesis Key reagents: Benzophenone, 4-</p>	AIE	ACN/buffer (1:9, v:v, pH 10)	373 nm; 540 nm ↑	0-100 μM; 0.1 μM	No	Yes	No	10

	<p>aminobenzophenone, salicylaldehyde, Zn, 4-(Bromomethyl)- benzene boronic acid pinacol ester, HCl, H₂O₂. Media: EtOH.</p>								
8	<p>2-steps synthesis from TPE-OH-CHO Key reagents: 4-bromobenzoyl chloride, AlCl₃, TiCl₄, Zn, NBS, bis(pinacolato)diboron, Pd(dppf)Cl₂. Media: Toluene, THF, DMSO, CCl₄, Dioxane.</p>	AIE	DMSO/PBS buffer (1:49, v:v)	430 nm; 576 nm ↑	60-300 μM; 3.2 μM	No	No	No	11
9	<p>2-steps synthesis for precursor compound followed</p>	AIE	Phosphate buffer	365 nm; 460 nm ↓	0.01-1.0 μM; 0.01 μM	No	Yes	No	12

	<p>by L-cys addition</p> <p>Key reagents: (2-bromoethene-1,1,2-triyl)tribenzene, 4-aminophenyl boronic acid, furan-2,5-dione, Pd(PPh₃)₄.</p> <p>Media: THF, CHCl₃, acetic anhydride.</p>								
10	 <p>2-steps synthesis</p> <p>Key reagents: 2-(benzo[d]oxazol-2-yl)-4-nitrophenol, 4-(Bromomethyl)- benzene boronic acid pinacol ester, 1,1'-carbonyldiimidazole.</p> <p>Media: DMF.</p>	AIE, ESIPT	HEPES/ CTAB	385 nm; 405 nm ↓, 510 nm ↑	NA	No	No	No	13

11	 <p>2-steps synthesis</p> <p>Key reagents: N,N-dimethylaminobenzaldehyde, 4-bromophenylacetonitrile, bis(pinacolato)diboron, Pd(PPh₃)₂Cl₂.</p> <p>Media: Toluene, MeOH.</p>	AIEE	EtOH:HEPES (1:99)	381 nm; 516 nm ↓	NA; 0.45 μM	No	Yes	Industrial sample	14
12	 <p>3-steps synthesis</p> <p>Key reagents: Carbazole, ethyl acrylate, DMF, 1-ethyl-4-methylquinolin-1-ium iodide, POCl₃.</p> <p>Media: DMF.</p>	AIE	Tris-HCl buffer	517 nm; 615 nm ↑	4-5000 μM; 0.4 μM	No	No	No	15

13	 <p>4-steps synthesis</p> <p>Key reagents: 5-chlorosalicylaldehyde, thiophenol, benzophenone, 4-bromomethyl-benzene boronic acid, HMTA.</p> <p>Media: Solventless synthesis.</p>	AIE, ESIPT, TICT	DMSO/PBS buffer (01:99, v:v)	384 nm; 617 nm ↑	0-1.0 μM; 0.039 μM;	Yes	Yes	river water and blood serum samples	This work
----	---	------------------------	------------------------------------	---------------------------	------------------------	-----	-----	--	------------------

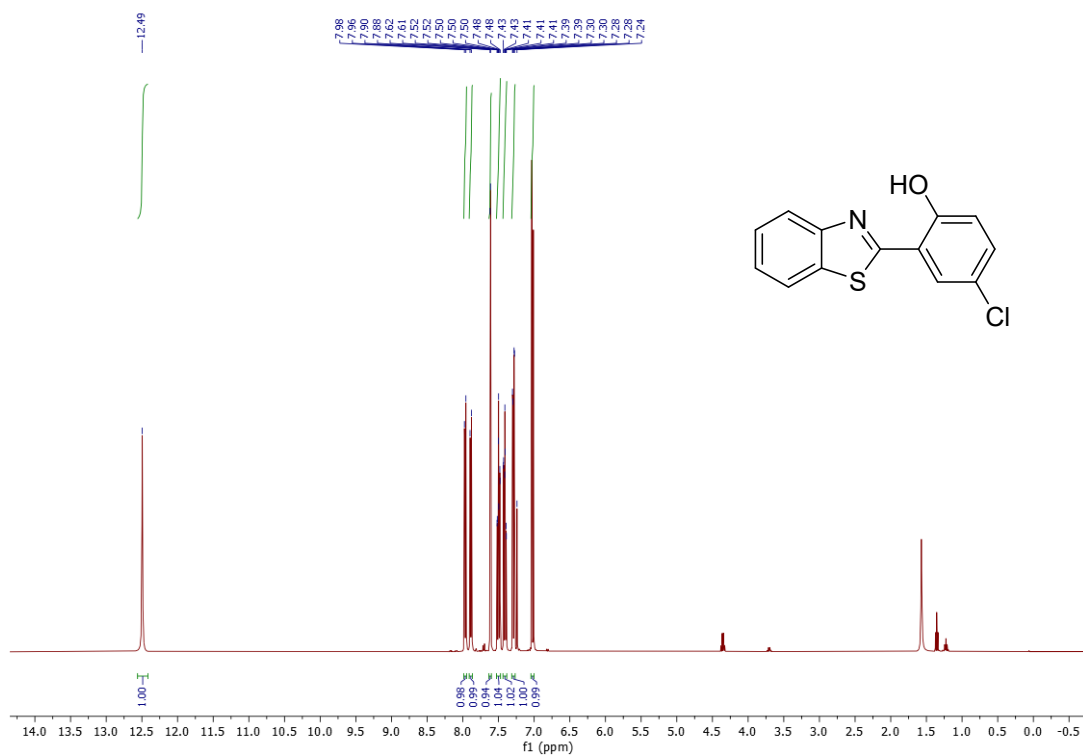
16. References:

1. P. Majumdar and J. Zhao, 2-(2-Hydroxyphenyl)-benzothiazole (HBT)-rhodamine dyad: Acid-switchable absorption and fluorescence of excited-state intramolecular proton transfer (ESIPT), *J. Phys. Chem. B* 2015, **119**, 2384–2394, <https://doi.org/10.1021/jp5068507>.
2. T. Peng, N. -K. Wong, X. Chen, Y. -K. Chan, D. H. -H. Ho, Z. Sun, J. J. Hu, J. Shen, H. El-Nezami and D. Yang, Molecular imaging of peroxyxynitrite with HKGreen-4 in live cells and tissues, *J. Am. Chem. Soc.* 2014, **136**, 11728–11734, <https://doi.org/10.1021/ja504624q>.
3. V. G. Naik, V. Kumar, A. C. Bhasikuttan, K. Kadu, S. R. Ramanan, A. A. Bhosle, M. Banerjee and A. Chatterjee, Solid-supported amplification of aggregation emission: a tetraphenylethylene-cucurbit[6]uril@hydroxyapatite-based supramolecular sensing assembly for the detection of spermine and spermidine in human urine and blood, *ACS Appl. Bio Mater.* 2021, **4**, 1813–1822, <https://doi.org/10.1021/acsabm.0c01527>.
4. J. Xu, Y. Zhang, H. Yu, X. Gao and S. Shao, Mitochondria-targeted fluorescent probe for imaging hydrogen peroxide in living cells, *Anal. Chem.* 2016, **88**, 1455–1461, <https://doi.org/10.1021/acs.analchem.5b04424>.
5. L. Xu, Y. Zhang, L. Zhao, H. Han, S. Zhang, Y. Huang, X. Wang, D. Song, P. Ma, P. Ren and Y. Sun, A neoteric dual-signal colorimetric fluorescent probe for detecting endogenous/exogenous hydrogen peroxide in cells and monitoring drug-induced hepatotoxicity, *Talanta* 2021, **233**, 122578, <https://doi.org/10.1016/j.talanta.2021.122578>.
6. E. Lindberg and N. Winssinger, High Spatial resolution imaging of endogenous hydrogen peroxide in living cells by solid-state fluorescence, *ChemBiochem* 2016, **17**, 1612–1615, <https://doi.org/10.1002/cbic.201600211>.
7. D. Liu, G. Chen and G. Fang, A near-infrared, colorimetric and ratiometric fluorescent sensor

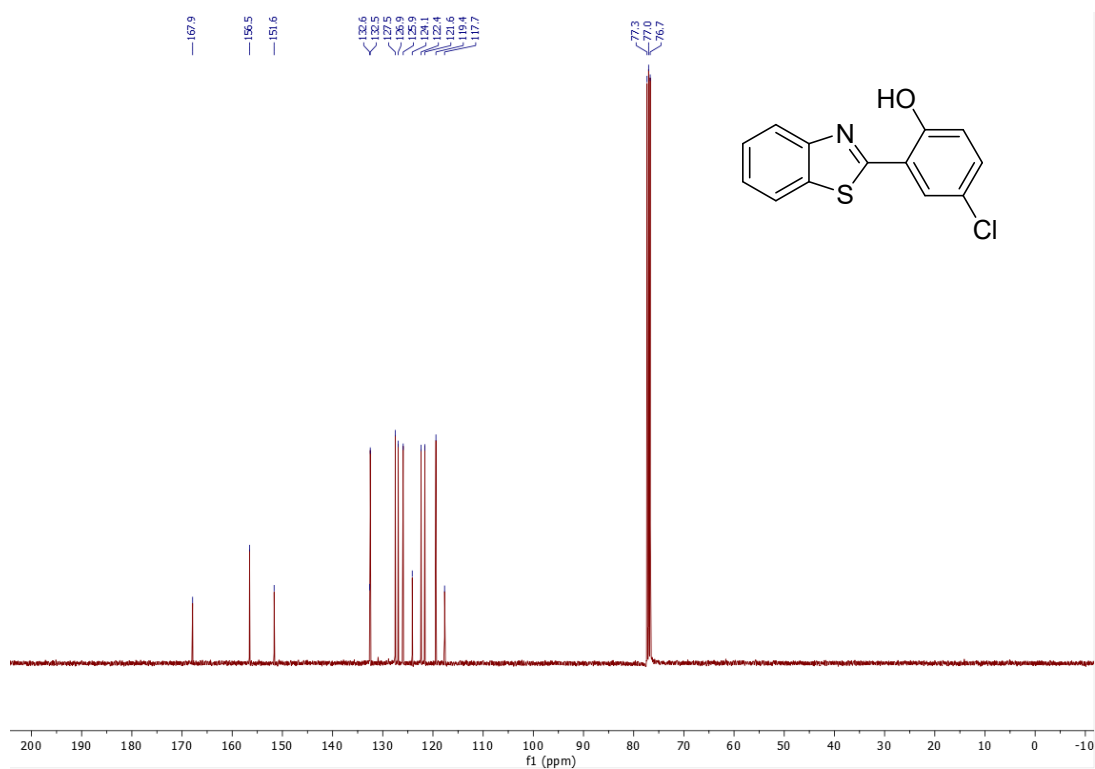
- with high sensitivity to hydrogen peroxide and viscosity for solutions detection and imaging living cells, *Bioorg. Chem.* 2022, **119**, 105513, <https://doi.org/10.1016/j.bioorg.2021.105513>.
8. W. Zhang, W. Liu, P. Li, F. Huang, H. Wang and B. Tang, Rapid-response fluorescent probe for hydrogen peroxide in living cells based on increased polarity of C-B bonds, *Anal. Chem.* 2015, **87**, 9825–9828, <https://doi.org/10.1021/acs.analchem.5b02194>.
 9. Y. Liu, J. Nie, J. Niu, F. Meng and W. Lin, Ratiometric fluorescent probe with AIE property for monitoring endogenous hydrogen peroxide in macrophages and cancer cells, *Sci. Rep.* 2017, **7**, 7293, <https://doi.org/10.1038/s41598-017-07465-5>.
 10. Z. Song, R. T. K. Kwok, D. Ding, H. Nie, J. W. Y. Lam, B. Liu and B. Z. Tang, An AIE-active fluorescence turn-on bioprobe mediated by hydrogen-bonding interaction for highly sensitive detection of hydrogen peroxide and glucose, *Chem. Commun.* 2016, **52**, 10076–10079, <https://doi.org/10.1039/c6cc05049b>.
 11. G. -J. Liu, Z. Long, H. -J. Lv, C. -Y. Li and G. -W. Xing, A dialdehyde–diboronate-functionalized AIE luminogen: Design, synthesis and application in the detection of hydrogen peroxide, *Chem. Commun.* 2016, **52**, 10233–10236, <https://doi.org/10.1039/c6cc05116b>.
 12. J. Chang, H. Li, T. Hou, W. Duan and F. Li, Paper-based fluorescent sensor via aggregation induced emission fluorogen for facile and sensitive visual detection of hydrogen peroxide and glucose, *Biosens. Bioelectron.* 2018, **104**, 152-157, <https://doi.org/10.1016/j.bios.2018.01.007>.
 13. G. Li, D. Zhu, Q. Liu, L. Xue and H. Jiang, Rapid detection of hydrogen peroxide based on aggregation induced ratiometric fluorescence change, *Org. Lett.* 2013, **15**, 924–927, <https://doi.org/10.1021/ol4000845>.
 14. S. Dhoun, S. Kaur, P. Kaur and K. Singh, A cyanostilbene-boronate based AIEE probe for hydrogen peroxide—Application in chemical processing, *Sens. Actuators, B* 2017, **245**, 95–103, <https://doi.org/10.1016/j.snb.2017.01.143>.
 15. N. Wang, J. Su, Q. Deng, A. Liu, F. Qi, J. Zhang, L. Long, S. Kong, C. Liu and R. Tang, G-

quadruplex-lighted EVCP for the construction of ratiometric fluorescent sensors: Detection of hydrogen peroxide and oxidase substrate, *Dyes Pigm.* 2020, **177**, 108132, <https://doi.org/10.1016/j.dyepig.2019.108132>.

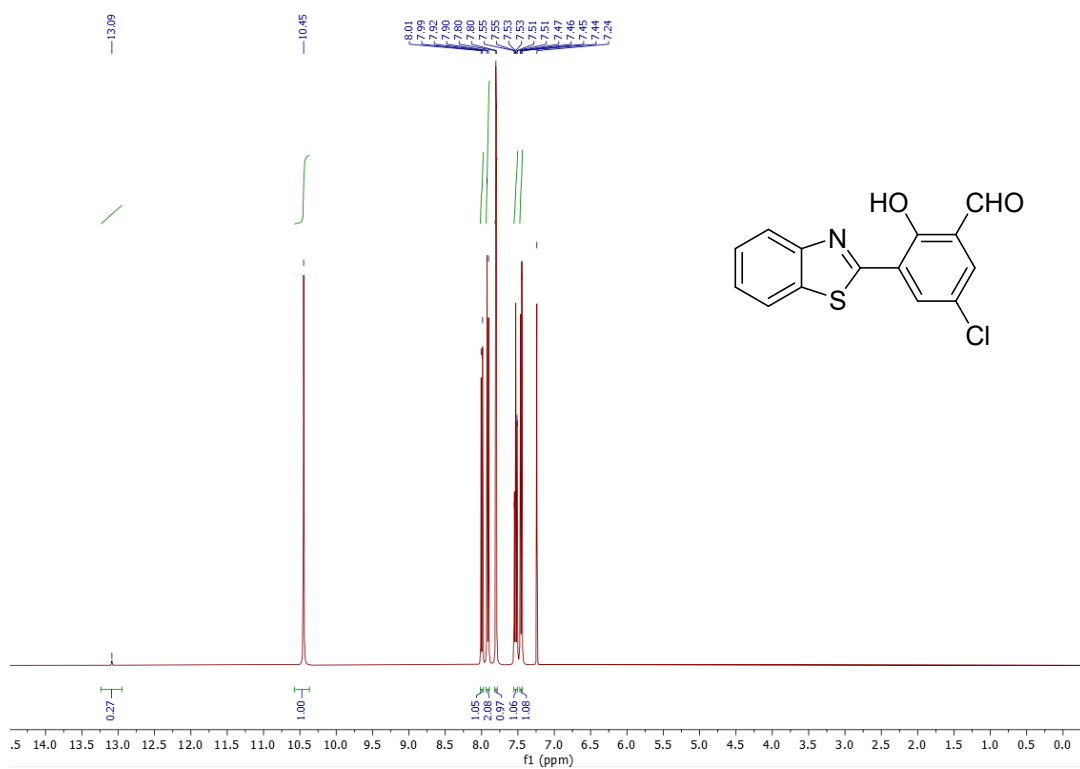
17. NMR Spectra:



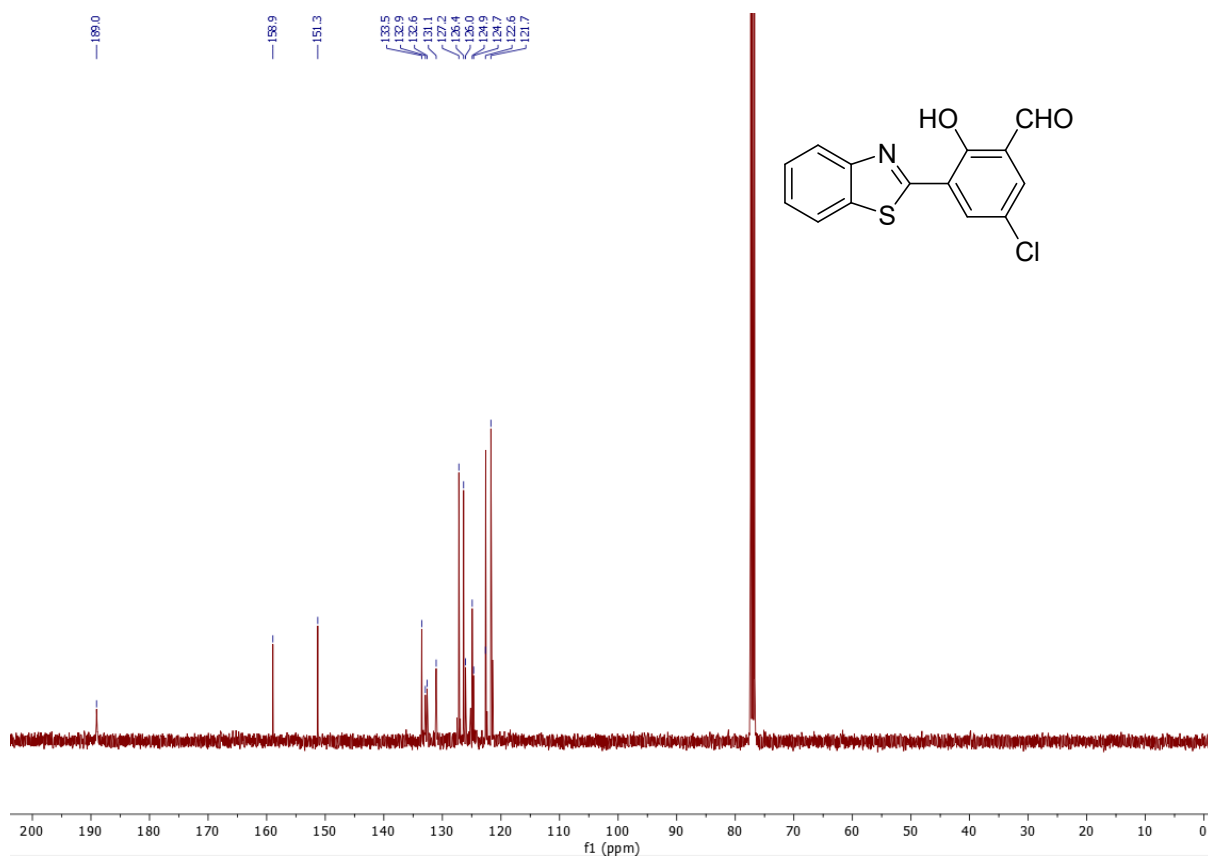
¹H NMR spectra of 2-(benzo[d]thiazol-2-yl)-4-chlorophenol (**1**).



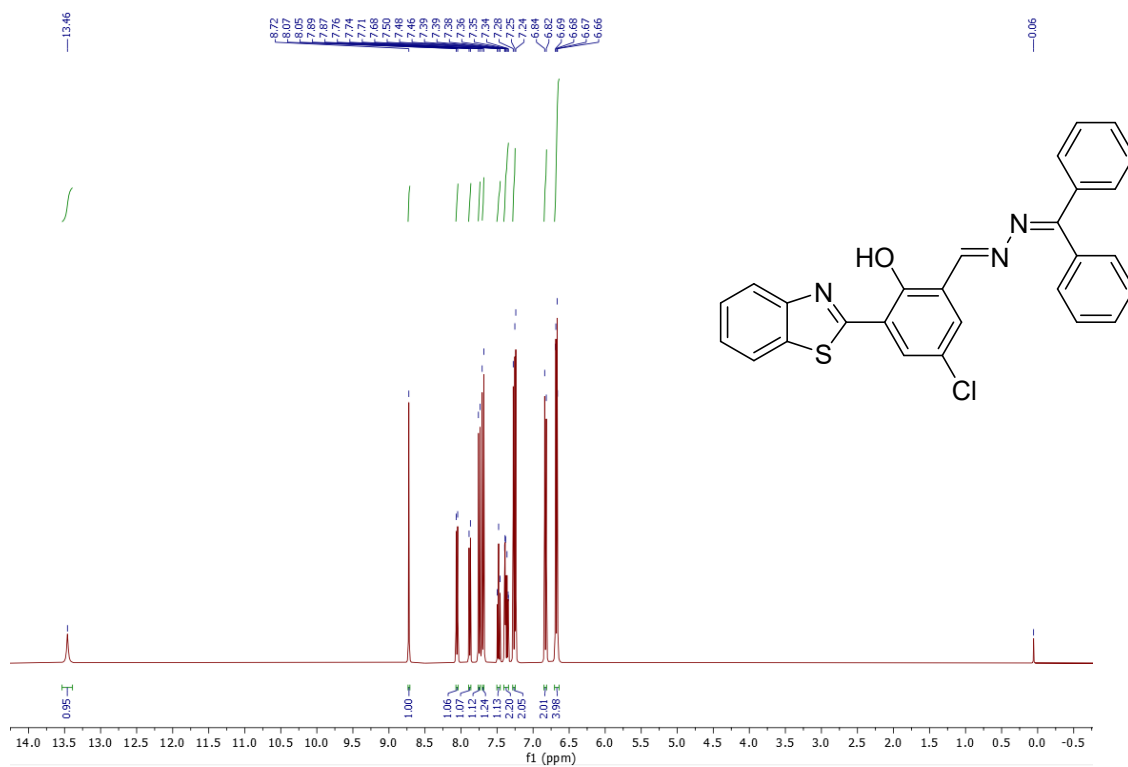
¹³C NMR spectra of 2-(benzo[d]thiazol-2-yl)-4-chlorophenol (**1**).



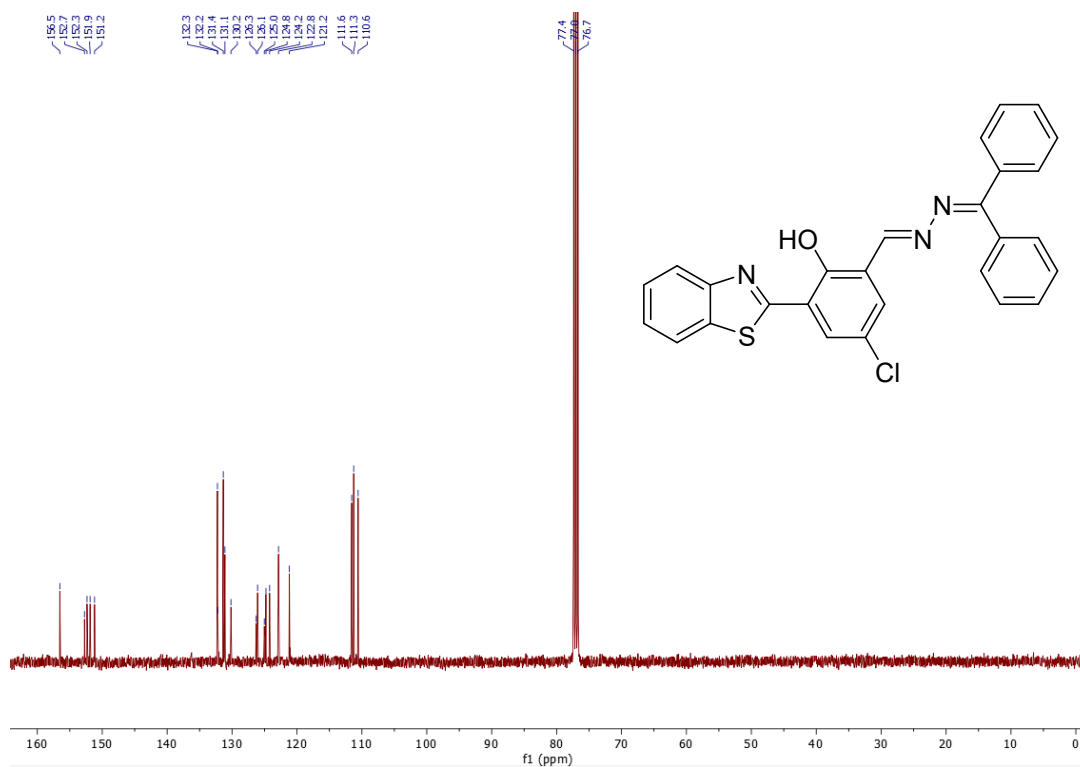
¹H NMR spectra of 3-(benzo[d]thiazol-2-yl)-5-chloro-2-hydroxybenzaldehyde (**2**).



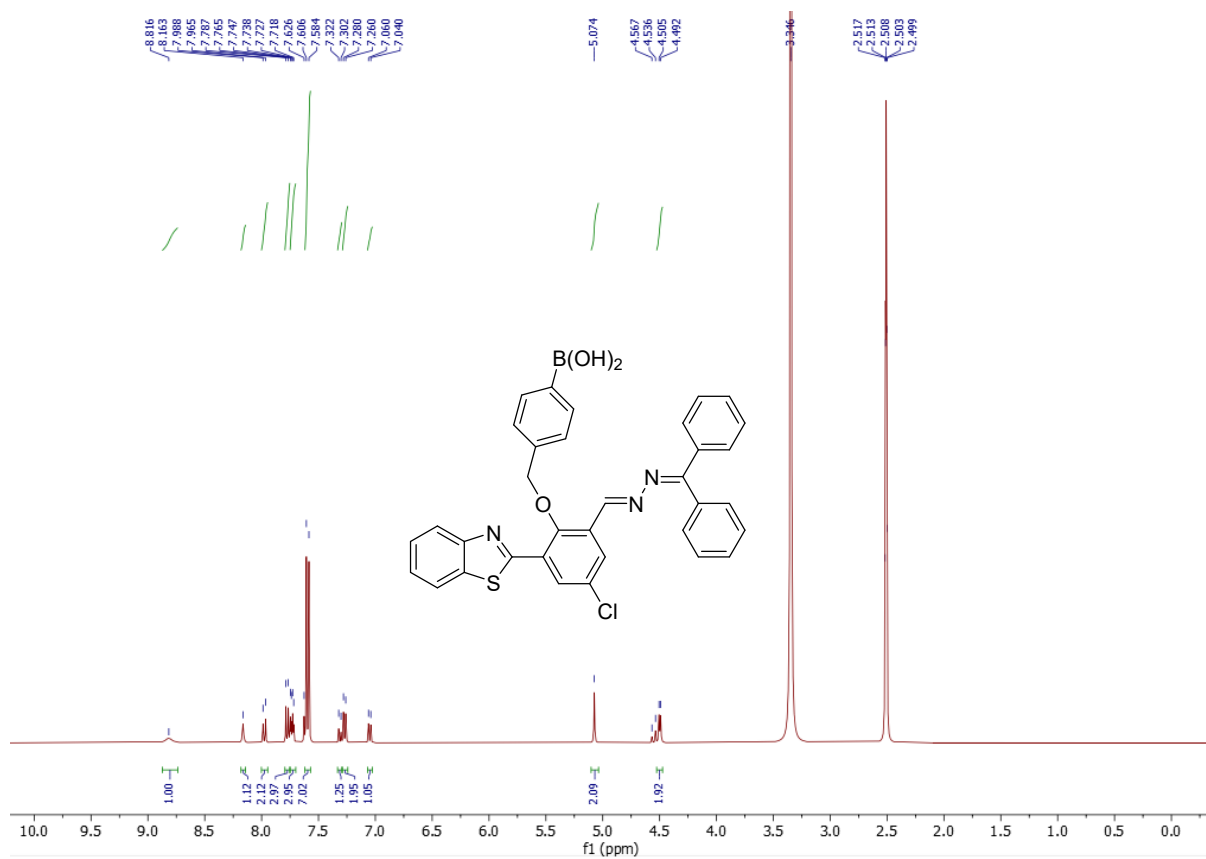
¹³C NMR spectra of 3-(benzo[d]thiazol-2-yl)-5-chloro-2-hydroxybenzaldehyde (**2**).



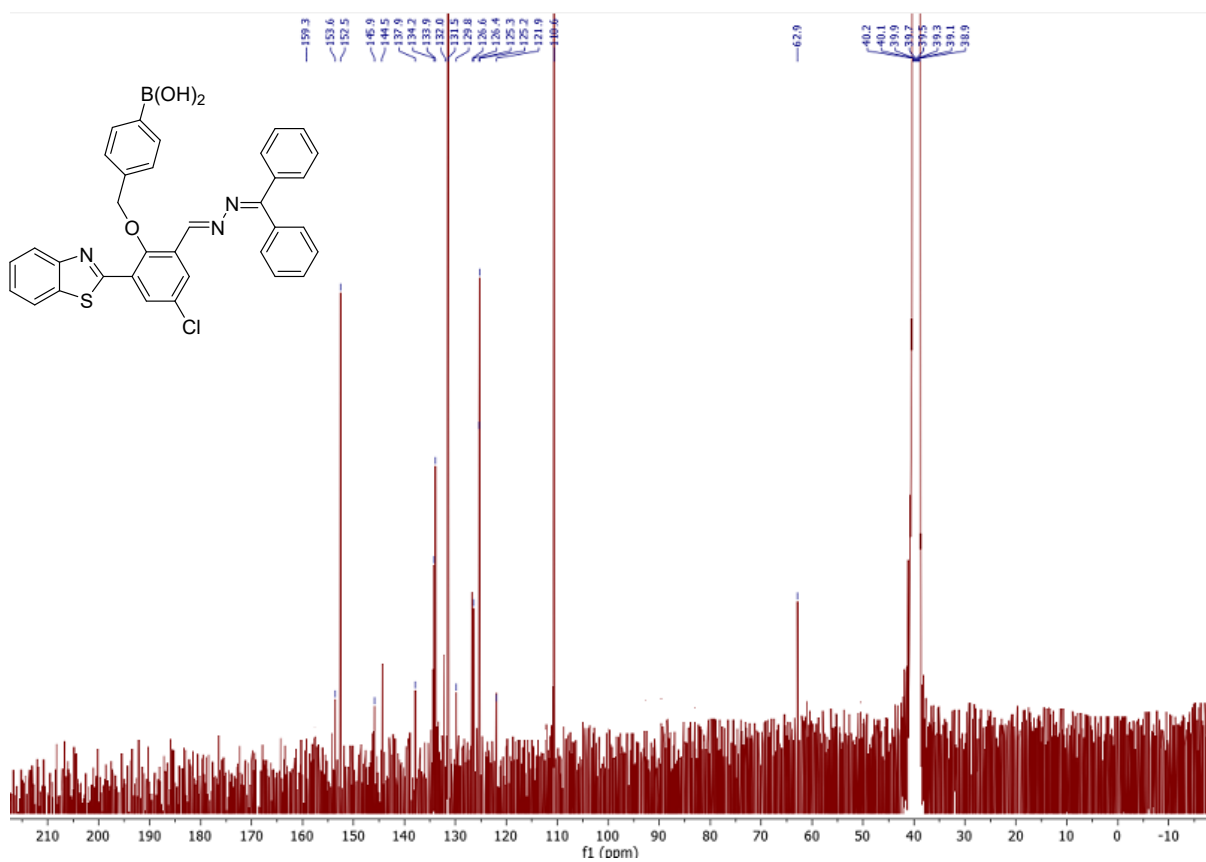
¹H NMR spectra of BTPA.



¹³C NMR spectra of BTPA.



¹H NMR spectra of BTPAB.



¹³C NMR spectra of BTPAB.